Emerging *Clostridioides difficile* ribotypes have divergent metabolic phenotypes

Firas S. Midani,[1,2] Heather A. Danhof,[1,2] Nathanael Mathew,[1,2] Colleen K. Ardis,[1,2] Kevin W. Garey,[3] Jennifer K. Spinler,[4] and Robert A. Britton[1,2,#]

[1]Alkek Center for Metagenomics and Microbiome Research, Baylor College of Medicine, Houston, Texas, USA
[2]Department of Molecular Virology and Microbiology, Baylor College of Medicine, Houston, Texas, USA
[3]Department of Pharmacy Practice and Translational Research, University of Houston, Houston, Texas, USA
[4]Department of Pathology and Immunology, Baylor College of Medicine, Houston, Texas, USA
[#] Address correspondence to Robert Britton, robert.britton@bcm.edu.

Running Title: Divergent metabolism of *C. difficile* ribotypes

Keywords: *Clostridioides difficile*, growth modeling, carbon metabolism, ribotyping.

Word Counts:185 (abstract) and 4,158 (text excluding references and figure legends).

ABSTRACT

Clostridioides difficile is a gram-positive spore-forming pathogen that commonly causes diarrheal infections in the developed world. Although *C. difficile* is a genetically diverse species, certain ribotypes are overrepresented in human infections. It is unknown if metabolic adaptations are essential for the emergence of these epidemic ribotypes. Here, we tested carbon substrate utilization by 88 *C. difficile* isolates and looked for differences in growth between 22 ribotypes. By profiling clinical isolates, we assert that *C. difficile* is a generalist species capable of growing on a variety of carbon substrates. Further, *C. difficile* strains clustered by phylogenetic relationship and displayed ribotype-specific and clade-specific metabolic capabilities. Surprisingly, we observed that two emerging lineages, ribotypes 023 and 255, have divergent metabolic phenotypes. In addition, although *C. difficile* Clade 5 is the most evolutionary distant clade and often detected in animals, it displayed more robust growth on simple dietary sugars than Clades 1-4. Altogether, our results corroborate the generalist metabolic strategy of *C. difficile* and demonstrate lineage-specific metabolic capabilities. In addition, our approach can be adapted to the study of additional pathogens to ascertain their metabolic niches in the gut.

IMPORTANCE

The gut pathogen *Clostridioides difficile* utilizes a wide range of carbon sources. Microbial communities can be rationally designed to combat *C. difficile* by depleting its preferred nutrients in the gut. However, *C. difficile* is

genetically diverse with hundreds of identified ribotypes and most of its metabolic studies were performed with lab-adapted strains. Here, we profiled carbon metabolism by a myriad of *C. difficile* clinical isolates. While the metabolic capabilities of these isolates clustered by their genetic lineage, we observed surprising metabolic divergence between two emerging lineages. We also found that the most genetically distant clade grew robustly on simple dietary sugars, posing intriguing questions about the adaptation of *C. difficile* to the human gut. Altogether, our results underscore the importance of considering the metabolic diversity of pathogens in the study of their evolution and the rational design of therapeutic interventions.

INTRODUCTION

Clostridioides difficile is a common cause of gastrointestinal infections with symptoms ranging from mild diarrhea to pseudomembranous colitis which can be fatal (1). By disrupting the gut microbiome, antibiotic use lessens microbial competition for nutrients in the gut and increases the risk of *C. difficile* infection (2). Although hospital-acquired *C. difficile* infections are decreasing likely due to better infection-prevention and antibiotic stewardship efforts, community-acquired *C. difficile* infections are increasing (3). Therefore, gut microbial alterations due to factors other than antibiotics may also increase the risk of *C. difficile* infections. As a strong driver of gut microbial composition (4), diet modulates the risk or severity of *C. difficile* infection in animals (5, 6), and dietary additives may have contributed to the emergence of epidemic *C. difficile* lineages (7). However, the contribution of the human diet to *C. difficile* epidemiology and pathogenesis remains incompletely understood.

As a generalist species, *C. difficile* occupies various nutritional niches in the human gut. Because it is adept at fermenting both amino acids and carbohydrates (8, 8), *C. difficile* thrives during antibiotic disturbance (2, 9), chronic inflammation (10), or toxin-induced inflammation (11, 12). However, this rich understanding of *C. difficile* metabolism was derived from animal studies using lab-adapted *C. difficile* strains, and confounded by the phenotypic divergence of the same *C. difficile* strain passaged in different laboratories (13). Additionally, *C. difficile* is a diverse species that has five well-defined phylogenetic clades (14) and at least 116 PCR ribotypes (15). Metabolic capabilities including fermentation of amino acids and central carbon metabolites also varied considerably between strains comprising the five major clades (16). Accordingly, it is unknown if clinical *C. difficile* isolates have similar metabolic capabilities as lab-adapted strains and whether dominant ribotypes have metabolic advantages over ribotypes that cause a lower burden of human infections.

Here, we address these issues by measuring and comparing the growth of 88 *C. difficile* isolates on a variety of carbon substrates. By profiling growth in Biolog Phenotype Microarray plates, we identified a wide range of carbon sources used by the *C. difficile* species and compared how ribotypes differentially grew on these substrates. We also contrasted the growth of the emerging ribotypes 023 and 255, and the growth of ancestral Clade 5 ribotypes to newer Clade 1-4 ribotypes. Altogether, our results expand our understanding of the metabolic diversity of *C. difficile* and pose new questions about the evolution of the *C. difficile* species.

RESULTS

Broad survey of carbon substrate utilization by various clinical *C. difficile* ribotypes

We profiled the growth of 88 *C. difficile* strains on 190 unique carbon substrates using Biolog Phenotype microarray plates. Tested strains comprised all five phylogenetic clades and at least 22 ribotypes. Strains

profiled were from patient samples (n=82) or lab-adapted isolates (n=6), including CD630, R20291, VPI 10463, and M68. Strains were grown anaerobically for 17 hours in Biolog plates which are pre-loaded with a single carbon substrate in each well. We estimated the maximum population size for each monoculture (carrying capacity) using the maximum change in optical density during the growth experiments. Because *C. difficile* grows in minimal media using Stickland fermentation of amino acids, maximum changes in optical density reflect the additive growth on amino acids in the minimal media and on the single carbon source pre-loaded in each well. We therefore adjusted the carrying capacities for each isolate by subtracting its carrying capacity on minimal media alone in the control well (normalized carrying capacity). This normalization allowed us to discriminate the contribution of a carbon source versus amino acids to bacterial growth, and account for variation in the growth of different isolates on minimal media.

C. difficile is a generalist species that grows on a variety of carbon substrates

C. difficile isolates grew on a variety of carbon substrates. Out of 190 tested carbon sources, 26 substrates increased optical density by at least 0.1 units for at least 10% of the tested isolates (**Figure 1**). To rank these substrates based on their contribution to *C. difficile* growth, we ordered them by their median normalized carrying capacities. *C. difficile* reached the highest biomass on simple sugars, followed by sugar derivatives, sugar alcohols, amino acids, then carboxylic acids. Conversely, our survey also revealed several substrates that decreased optical density by a mean of at least 0.05 units. These inhibitory substrates were dominated by acids and included substrates with known antimicrobial effects, such as capric acid, and those that can be microbially produced, such as phenylethylamine (17, 18).

C. difficile lineages are distinguished by phylogenetically conserved metabolic capabilities

Because *C. difficile* is a genetically diverse species with many ribotypes, we wondered if ribotypes cluster based on their carbon substrate utilization profiles. We performed a principal component analysis of the normalized carrying capacities for the top 26 carbon substrates. Isolates strongly clustered by phylogenetic clades for the first two principal components which collectively explained 56.9% of the variance (**Figure 2A,C**), and showed clustering by ribotype for the first four principal components, which collectively explained 73.8% of the variance (**Figure 2C-D**). Principal component loadings, which describe how substrates contribute to each principal component, showed that the clustering of both clades and ribotypes was mostly driven by 9 substrates (**Figure 2E-F**). These substrates were the sugars trehalose, mannose, ribose, and melezitose; the sugar derivatives arbutin and salicin; and the sugar alcohols sorbitol, mannitol, and arabitol. The direction of loadings aligned with the growth of ribotypes on each substrate (**Figure S1**). For example, trehalose supported the highest carrying capacities for isolates in Clades 2 and 5, and these are the isolates most positively correlated with trehalose loading on principal component 2. Likewise, Clade 5 and ribotype 015 isolates are unable to grow on melezitose and occupy the principal component space opposite the direction of the

melezitose loading on the first two principal components. In summary, genetically diverse isolates cluster by phylogenetic clade and ribotype based on their carbon substrate utilization.

Emerging ribotypes have divergent metabolic phenotypes

To determine how substrate utilization differentiates ribotypes, we compared the growth of ribotypes on carbon substrates that supported *C. difficile* growth. First, we grouped isolates into sets based either on ribotype or habitat (e.g., lab-adapted). For each substrate, isolates were then ranked based on their normalized carrying capacity. Next, we used strain set enrichment analysis (an approach akin to gene set enrichment analysis; see **Methods**) to compute an enrichment score that reflects the degree to which a strain set (group of isolates) is overrepresented at the extremes (top or bottom) of the entire ranked list of isolates. Our analysis focused on groups that were profiled with a minimum of 4 isolates and included the following groups: RT027+, RT014+, RT106+, RT255, RT023, RT017, RT078, Clade 5+ (i.e., non-RT078 isolates), and lab-adapted strains (CD630, R20291, VPI 10463, M68). Here, a "+" sign indicates that a group included closely related ribotypes. Our analysis showed that ribotypes 255, 027, and 017 are positively enriched (higher carrying capacities) while ribotypes 014-020, 106, and 023 are negatively enriched (lower carrying capacities) (**Figure 3**). Clade 5 ribotypes including ribotype 078 have a similar balance of positive and negative enrichments. Surprisingly, two emerging ribotypes displayed polarized enrichment patterns (**Figure 4A**). Ribotype 255 had 24 out of 26 positive enrichments with 9 of those being significant, while ribotype 023 had 20 out of 26 negative enrichments with 5 of those being significant (**Figure S2**). This divergence in enrichments suggests that a ribotype can emerge even if it grows poorly on many of the carbon sources commonly used by *C. difficile*.

Emerging ribotype 255 grows robustly on a variety of substrates

Ribotype 255 is an emerging *C. difficile* lineage that comprised approximately 2-5% of cases in the United States between 2016 and 2018 (19–21). We observed that ribotype 255 was significantly enriched on various substrates (**Figure 3**). Notably, ribotype 255 grew significantly higher than other ribotypes on minimal media supplemented with fructose or ribose (**Figure S3**). To verify these observations, we re-tested the growth of ribotype 255 and other isolates representing various common ribotypes on minimal media supplemented with fructose or ribose at multiple concentrations. Unlike Biolog assays, where cultures were started with inocula harvested from overnight cultures, we started cultures from inocula harvested during exponential growth and monitored growth for 24 hours. We observed significantly higher growth for ribotype 255 on fructose and ribose ($P < 0.05$**,** linear mixed effects model; **Figure 4B**). We repeated this assay with fewer isolates but more substrates. The order of ribotypes on fructose, mannitol, salicin, and ribose, recapitulated the patterns detected by our Biolog assays (**Figure S4**). Ribotype 255 grew to a higher density than ribotypes 027, 106, and 014 on fructose, mannitol, and ribose, while ribotype 255 had the worst growth on salicin. Notably, although overnight

cultures of ribotypes 017 and 078 were unable to grow on ribose in fresh media (**Figure S1**), these ribotypes grew on ribose when it was introduced during exponential growth.

Clade 5 ribotypes grow more robustly on simple sugars than Clade 1-4 ribotypes

Clade 5 is the most evolutionary distant *C. difficile* clade and includes ribotypes that are frequently detected in animals (22, 23). Comparative genomics suggested that the divergence of Clades 1-4 from Clade 5 is linked to positive selection on genes involved in metabolism of simple sugars (24). Therefore, we expected significant metabolic differences between Clades 1-4 and Clade 5, but we only observed modest differences in growth between these clade groups. Animal-associated ribotypes (Clade5+) were also distinguished only by increased growth on trehalose and sorbitol and decreased growth on glucose, N-acetyl-glucosamine, ethanolamine, and melezitose (**Figure 3**). To further investigate these observations, we compared the growth of Clade 5 ribotypes to Clades 1-4 ribotypes on eight different substrates including the simple sugars glucose, fructose, tagatose, and ribose (**Figure 5**). Cultures were started with mid-exponential growth inoculum and growth was monitored for 48 hours. For Clade 5 isolates, we included both human- and animal-associated ribotype 078 strains and animal-associated ribotypes 033, 126, and 288 strains. Surprisingly, Clade 1-4 isolates had significantly lower growth on simple sugars ($P < 0.001$, linear mixed effects model), although Clade 1-4 and Clade 5 isolates had similar growth overall ($P > 0.05$, linear mixed effects model). Indeed, substrate-specific comparisons showed that Clade 5 isolates grew to a significantly higher density on ribose and tagatose ($P < 0.05$, linear mixed effects model). In summary, Clade 5 ribotypes grew more robustly on simple sugars than common ribotypes in Clades 1-4.

Gene-environment interactions are necessary for growth on certain substrates

We previously showed that ribotypes 027, 078, and 017 encode genetic variants or operons that facilitate competitive growth on trehalose (7, 25). Here, we observed that ribotypes 017 isolates, which have a C171S amino acid substitution in the trehalose operon repressor *treR* (25), did not grow on trehalose in our Biolog assay. So, we re-tested M68, a ribotype 017 reference strain, on Biolog Phenotype Microarray plates using different growth media for its overnight culture, before dilution and inoculation into Biolog plates. M68 was able to grow on trehalose when its inoculum was cultured overnight on brain-heart infusion media supplemented with high (5%) but not low (0.5%) yeast extract (**Figure 6**). We hypothesized that high yeast extract in overnight culture provided a limiting growth cofactor for trehalose metabolism by ribotype 017. To test this, we reasoned that cell cultures that are either washed or highly diluted before inoculating into minimal media would not retain the unknown growth factor and would not be able to grow on trehalose. Indeed, we observed that M68, which was pre-grown overnight on BHI with high yeast extract, was unable to grow on trehalose as the sole carbon source if it had been washed or highly diluted before inoculation (**Figure S5A**). In contrast, CD2015, a ribotype 027 isolate, was able to grow on trehalose even after both washing and dilution (**Figure**

S5B). Altogether, this precarious growth of M68 suggests that an unknown limiting factor can modify the growth of some *C. difficile* strains on certain substrates, including trehalose, ribose, and cellobiose.

DISCUSSION

By identifying the metabolic needs and preferences of *C. difficile*, we can begin to inform the design of microbial and dietary interventions for the prevention and treatment of *C. difficile* infections. Indeed, microbial communities can be rationally designed to resist *C. difficile* by blocking access to key nutrients (26, 27), and dietary alterations can prevent enteric infections (28). Here, we expand our metabolic understanding of *C. difficile* by profiling carbon substrate utilization of clinical isolates comprising all five major clades. Our results corroborate that *C. difficile* is a bacterial generalist that can grow on a wide array of carbon sources, and that common *C. difficile* lineages exhibit unique metabolic capabilities. Surprisingly, we observed divergent metabolic profiles for emerging ribotypes 023 and 255, and robust growth of the evolutionary distant Clade 5 on simple sugars. Altogether, our findings underscore the importance of considering the metabolic diversity of *C. difficile* in the design of microbial and dietary interventions.

Our results also highlight several carbohydrates that are variably used by *C. difficile* lineages and may be crucial in the design of dietary interventions. We have previously shown that trehalose metabolism is variable between ribotypes and that increased use of trehalose in food manufacturing correlated with the emergence of ribotypes that are highly adept at consuming trehalose (7, 25). In contrast, sugar alcohols are derived in the intestines from both the host metabolism and the diet. In mouse models of *C. difficile* infections, sugar alcohols were highly abundant in guts of susceptible animals (29), and sorbitol utilization genes were highly upregulated during *C. difficile* toxin-induced inflammation (12). Because sorbitol comprises the most used non-nutritive sweetener globally (30, 31), it is likely more common in the human diet than trehalose. Ribose is also highly abundant in the gut because it comprises the backbone of nucleobases. Importantly, gut commensals have adapted to sense and scavenge ribose from dietary nucleosides (32) and ribose transport and metabolism are highly expressed in mice mono-colonized with *C. difficile* (33). Additional studies are needed to verify the role of these nutrients in *C. difficile* colonization and pathogenesis.

By profiling the growth of all five major clades, our study also tested prevailing hypotheses about the evolution of the *C. difficile* species. A large-scale genomic analysis suggested that the divergence of Clades 1-4 from Clade 5 is linked to the metabolism of dietary simple sugars, and a related mouse experiment showed that fructose and glucose could differentially impact colonization of Clades 1-4 (24). However, this mouse experiment was biased by testing only two strains, Clade 2 R20291 and Clade 5 M120, which are both lab-adapted. In contrast, we showed that ancestral Clade 5 isolates are just as capable as newer Clade 1-4 isolates in terms of growth on simple sugars. Further, the two emerging lineages, ribotypes 255 and 023 which are in Clades 1 and 3 respectively (20, 34), had divergent metabolic phenotypes especially in terms of growth

on simple sugars. While these findings highlight the need for more representation of a pathogen's diversity in animal studies, it remains possible that simple sugars differentially impact the growth of newer *C. difficile* lineages in the gut.

Our results also emphasize that genomic potential does not always translate to metabolic activity. We previously showed that certain ribotypes can utilize trehalose at ultra-low concentrations due to unique gene variants or operons. These genetic signatures were also shown to be encoded in additional ribotypes (35), but it is unclear if the presence of these gene variants is sufficient for growth on trehalose. For example, while ribotype 023 lacks the canonical *treRA* operon, it encodes an alternative four-gene operon (35, 36) that grants ribotype 078 (and other Clade 5 isolates) the ability to grow on 10 mM trehalose (7). Yet, we were unable to grow ribotype 023 isolates even at higher concentrations of trehalose, possibly because of a truncation in *treX* (36). Similarly, we have previously shown that ribotype 017 isolates can grow on trehalose (25), but replication of this growth required an unknown limiting factor available in yeast extract.

Despite the evidence presented here, metabolic capabilities by clinical *C. difficile* isolates still need to be further studied. Our analysis was limited to the 190 carbon substrates included in the Biolog Phenotype Microarray plates. Also, these substrates are seeded in these plates at unknown proprietary concentrations which may result in missing interesting patterns, including the ability of certain ribotypes to grow on low levels of substrates such as trehalose (7). Moreover, we profiled growth using a specific growth protocol, and results may not generalize to different experimental conditions. For example, Clade 5 isolates were able to robustly grow on ribose if exposed to it during mid-exponential but not after overnight growth. Finally, Stickland fermentation of amino acids is crucial for *C. difficile* pathogenesis (8, 37–39), but our assay does not adequately discern the growth contribution of amino acids in the Biolog plates from amino acids in the minimal media. Although amino acids were the sole nitrogen source in our minimal media, they were also fermented as carbon sources by *C. difficile*. A defined growth medium that minimizes amino acids is necessary to properly investigate Stickland fermentation, as has been developed for the study of the Wood-Ljungdahl pathway in *C. difficile* (40).

Ultimately, our comprehensive study of carbon source utilization shows that clinical *C. difficile* isolates are bacterial generalists with lineage-specific metabolic adaptations. It remains unclear if these adaptations have contributed to the emergence of certain lineages or if they provide a competitive advantage in the human gut. Further, our results suggest the existence of unknown factors that are necessary for the growth of specific *C. difficile* lineages in certain nutritional environments. The discovery of these growth factors presents new opportunities to understand and control the engraftment of *C. difficile*. Finally, our analytical approach for comprehensively profiling the metabolic capacities of *C. difficile* can be adapted for the study of additional pathogens to discover insights about their metabolic needs in the gut.

MATERIALS AND METHODS

Bacterial strains

Clinical *C. difficile* strains were isolated from a variety of sources including patients in the United States (n=62), the Netherlands (n=6), Colombia (n=5), Japan (n=4), Australia (n=2), Czech Republic (n=1), Spain (n=1), and the United Kingdom (n=1). Lab-adapted *C. difficile* strains included R20291, CD630, VPI 10463, and M68. **Tables S1-2** describe the source and molecular typing of these isolates respectively. Notably, ribotype 255 strains were isolated from patients in the state of Texas by Kevin Garey's lab, while ribotype 023 strains were isolated from patients in various European sites by the labs of Ed Kuijper and Brendan Wren.

Bacterial growth assays

All preparation of bacterial strains and growth of bacterial cultures were performed under an anaerobic atmosphere (5% CO2, 5% H2, 90% N2) inside a vinyl anaerobic chamber (Coy Laboratory Products). Bacterial strains were revived from frozen stocks by streaking on brain heart infusion agar supplemented with 0.5% yeast extract then growing at 37C.

Biolog Phenotype Microarrays assays

Colonies on agar plates were cultured overnight for approximately 15-18 hours in BHIS broth, which is brain heart infusion media supplemented with 5% yeast extract. Cell cultures were then diluted 1:10 in a defined minimal media, which is a basal defined medium adapted from Table 1 of Karasawa et al. (41) with several adjustments (**Table S3**). Each well in the pre-reduced Biolog Phenotype Microarray plates were then filled with 100 µl of the diluted cell cultures. Plates were sealed with gas-permeable film then incubated in a microplate reader (Sunrise by Tecan Life Sciences or AccuSkan by Thermo Scientific) for 17 hours. Optical density (620 nm) was measured every 10 minutes immediately after 5 seconds of orbital shaking. The growth profiles for isolates were repeated at least twice except for two isolates, a Ribotype 106 isolate and another of unknown ribotype, which were measured only once.

Bacterial growth validation assays

Overnight cultures in BHIS broth were subcultured 1:5 in fresh media and grown to mid-exponential phase (OD ~0.6), then diluted 1:50 in defined minimal media. Cell suspensions were mixed 1:1 with twice-concentrated substrate solutions which were prepared in double-deionized water then filter-sterilized (0.22 µm pore size). Each well had a final volume of 200 ul of cell cultures which were gown statically for 24 hours in a microplate reader (Sunrise by Tecan Life Sciences). Optical density (620 nm) was measured every 10 minutes

immediately after 5 seconds of orbital shaking. For validation of M68 and CD2015 growth on trehalose, overnight cultures were washed inside the anaerobic chamber by spinning at 2,000 g for 2 minutes with a pulse centrifuge, decanting the supernatant, then resuspending pellets in defined minimal media.

Microbial growth curve analysis

The "AMiGA" software was used for analysis of growth curves collected in this study (42). To flag wells with growth issues, we used the "summarize" command by AMiGA to generate 96-well growth curve plots. We manually flagged wells where growth curves displayed either rapid spikes or dips in optical density (often caused by gas bubbles), high background noise (as determined by starting OD), or unusual noisy fluctuations in optical density. Plates that included a large number of flagged wells were excluded from analysis. Because growth curves of *C. difficile* do not always follow the classical logistic growth dynamics, we modeled growth curves using Gaussian Process regression with the "fit" command by AMiGA which estimated growth metrics including area under the curve, carrying capacity, and growth rates. Because *C. difficile* can grow in defined minimal media using Stickland fermentation of amino acids, we wanted to compare the growth dynamics of each *C. difficile* isolate on different substrates relative to its own growth on minimal media. Therefore, we computed the difference in each growth metric relative to its median value during growth on minimal media, either using the "normalize" command by AMiGA or custom-written Python script.

Principal Component Analysis

To see if isolates cluster by molecular ribotype or phylogenetic identity, we performed principal component analysis on the normalized carrying capacity for the top 26 substrates used by *C. difficile*. These top substrates increased the carrying capacity by an OD of 0.1 (relative to carrying capacity on minimal media) for at least 10% (i.e., 8) of the tested *C. difficile* isolates. Principal component analysis was performed using "statsmodels" Python package on zero-centered normalized carrying capacities. Using principal component loadings, we compared the contribution of each substrate to the position of an isolate on each principal component. We visualized the loadings only for substrates that were ranked in the top 5 in terms of loadings for each of the first four principal components.

Strain Set Enrichment Analysis

We devised a statistical approach that we termed strain set enrichment analysis (SSEA) in order to identify whether a *C. difficile* lineage can use certain substrates better or worse on average than other lineages. SSEA is methodologically similar to gene set enrichment analysis (GSEA). Whereas GSEA tests how sets of genes are enriched or depleted in terms of expression on a specific experimental condition (43), SSEA tests how sets of isolates (e.g. clades, ribotypes, or other arbitrary grouping) are enriched or depleted in terms of normalized

carrying capacity on a specific substrate. Strain set enrichment analysis was implemented using the "prerank" function by "gseapy" Python package (44). For this analysis, we only included sets with a minimum size of four, weighted enrichment scores by a value of 0.5, and estimated p-values with 10,000 permutations. *P* values were adjusted with Benjamni-Hocheberg false discovery rate correction.

Linear Mixed Effects Models

We ran linear mixed effects models, using the "lme4" R package, to determine the effect of different substrates and molecular identities on the growth of *C. difficile* isolates. *P* values were obtained by likelihood ratio tests using the "anova" function between two models which only differ by the inclusion of the fixed effects of interest. For evaluating the growth of ribotype 255 isolates on fructose and ribose (**Figure 4B**), likelihood ratio tests compared the full model (Carrying capacity ~ Ribotype_255:Substrate + Ribotype_255 + Substrate + Substrate_Concentration + 1|Isolate) with several reduced models. Comparison determined that both ribotype and ribotype:susbtrate interaction terms significantly affected carrying capacity. For evaluating the growth of Clade 5 isolates on simple sugars (**Figure 5**), likelihood ratio tests compared the full model (Carrying capacity ~ Clade_5:Substrate_Type + Substrate_Type + Clade_5 + Substrate + 1|Isolate) with a reduced model that omitted the interaction term. Comparison determined that the interaction of Clade_5 with substrate type significantly affected carrying capacity. We also tested the differential growth between Clade 5 and Clades 1-4 on each substrate by comparing the full model (Carrying capacity ~ Clade_5 + Substrate + 1|Isolate) with a reduced model that omitted the Clade_5 term. These substrate-specific analyses identified significantly higher growth for Clade 5 on ribose and tagatose.

Data and code availability

Microplate reader data is available at https://doi.org/10.5281/zenodo.12626878. Code for analyzing data and creating figures is available at https://github.com/firasmidani/cdiff-biolog-growth. The full list and versions of computational tool used for data analysis is included in the GitHub repository.

ACKNOWLEDGEMENTS

We would like to thank the following for collecting or providing *C. difficile* isolates that were profiled in this study: Ed Kuijper (Leiden University), Brendan Wren (London School of Hygiene and Tropical Medicine), Angel Augusto Gonzalez Marin (Universidad de Antioquia), Haru Kato and Mitsutoshi Senoh (National Institute of Infectious Diseases, Tokyo, Japan), Sara McNamara (Michigan Department of Community Health), Joseph Sorg (Texas A&M University), and Dena Lyras (Monash University). We also thank Lei Pan and James Collins for processing six strains with Biolog phenotype microarray plates and Eva Preisner for sharing related data.

This research was supported by several NIH grants: F.S.M acknowledges support from T32DK007664, H.A.D. acknowledges support from F32AI136404, and R.A.B. acknowledges support from U19AI157981, R01AI123278, and U01AI124290. Data analysis was performed on the HPC cluster that is managed by the Biostatistics and Informatics Shared Resource (BISR) and supported by an NCI P30-CA125123 and Institutional funds from the Dan L Duncan Comprehensive Cancer Center and Baylor College of Medicine.

AUTHOR CONTRIBUTIONS

FSM and RAB conceptualized the study; FSM and HAD administered the study; FSM, HAD, and RAB developed methods; KWG and JKS provided bacterial strains; JKS sequenced isolates; FSM, HAD, NM, and CKA performed growth experiments; FSM and NM performed validation experiments; FSM developed software, analyzed data, curated data, and visualized results; RAB and KWG acquired funding; RAB supervised the project; FSM wrote the manuscript; and all authors reviewed and edited the manuscript.

CONFLICT OF INTEREST

Authors declare no conflicts of interest.

REFERENCES

1. Smits WK, Lyras D, Lacy DB, Wilcox MH, Kuijper EJ. 2016. Clostridium difficile infection. Nat Rev Dis Primers 2:16020.

2. Jenior ML, Leslie JL, Young VB, Schloss PD. 2017. Clostridium difficile Colonizes Alternative Nutrient Niches during Infection across Distinct Murine Gut Microbiomes. mSystems 2.

3. Guh AY, Mu Y, Winston LG, Johnston H, Olson D, Farley MM, Wilson LE, Holzbauer SM, Phipps EC, Dumyati GK, Beldavs ZG, Kainer MA, Karlsson M, Gerding DN, McDonald LC. 2020. Trends in U.S. Burden of *Clostridioides difficile* Infection and Outcomes. N Engl J Med 382:1320–1330.

4. David LA, Maurice CF, Carmody RN, Gootenberg DB, Button JE, Wolfe BE, Ling AV, Devlin AS, Varma Y, Fischbach MA, Biddinger SB, Dutton RJ, Turnbaugh PJ. 2014. Diet rapidly and reproducibly alters the human gut microbiome. Nature 505:559–563.

5. Hryckowian AJ, Van Treuren W, Smits SA, Davis NM, Gardner JO, Bouley DM, Sonnenburg JL. 2018. Microbiota-accessible carbohydrates suppress Clostridium difficile infection in a murine model. Nat Microbiol 3:662–669.

6. Mefferd CC, Bhute SS, Phan JR, Villarama JV, Do DM, Alarcia S, Abel-Santos E, Hedlund BP. 2020. A High-Fat/High-Protein, Atkins-Type Diet Exacerbates Clostridioides (Clostridium) difficile Infection in Mice, whereas a High-Carbohydrate Diet Protects. mSystems 5.

7. Collins J, Robinson C, Danhof H, Knetsch CW, van Leeuwen HC, Lawley TD, Auchtung JM, Britton RA. 2018. Dietary trehalose enhances virulence of epidemic Clostridium difficile. Nature 553:291–294.

8. Neumann-Schaal M, Jahn D, Schmidt-Hohagen K. 2019. Metabolism the Difficile Way: The Key to the Success of the Pathogen Clostridioides difficile. Front Microbiol 10:219.

9. Jenior ML, Leslie JL, Young VB, Schloss PD. 2018. *Clostridium difficile* Alters the Structure and Metabolism of Distinct Cecal Microbiomes during Initial Infection To Promote Sustained Colonization. mSphere 3:e00261-18.

10. Bushman FD, Conrad M, Ren Y, Zhao C, Gu C, Petucci C, Kim M-S, Abbas A, Downes KJ, Devas N, Mattei LM, Breton J, Kelsen J, Marakos S, Galgano A, Kachelries K, Erlichman J, Hart JL, Moraskie M, Kim D, Zhang H, Hofstaedter CE, Wu GD, Lewis JD, Zackular JP, Li H, Bittinger K, Baldassano R. 2020. Multi-omic Analysis of the Interaction between Clostridioides difficile Infection and Pediatric Inflammatory Bowel Disease. Cell Host & Microbe 28:422-433.e7.

11. Fletcher JR, Pike CM, Parsons RJ, Rivera AJ, Foley MH, McLaren MR, Montgomery SA, Theriot CM. 2021. Clostridioides difficile exploits toxin-mediated inflammation to alter the host nutritional landscape and exclude competitors from the gut microbiota. Nat Commun 12:462.

12. Pruss KM, Sonnenburg JL. 2021. C. difficile exploits a host metabolite produced during toxin-mediated disease. Nature 593:261–265.

13. Norsigian CJ, Danhof HA, Brand CK, Oezguen N, Midani FS, Palsson BO, Savidge TC, Britton RA, Spinler JK, Monk JM. 2020. Systems biology analysis of the Clostridioides difficile core-genome contextualizes microenvironmental evolutionary pressures leading to genotypic and phenotypic divergence. npj Syst Biol Appl 6:31.

14. Knight DR, Imwattana K, Kullin B, Guerrero-Araya E, Paredes-Sabja D, Didelot X, Dingle KE, Eyre DW, Rodríguez C, Riley TV. 2021. Major genetic discontinuity and novel toxigenic species in Clostridioides difficile taxonomy. eLife 10:e64325.

15. Stubbs SLJ, Brazier JS, O'Neill GL, Duerden BI. 1999. PCR Targeted to the 16S-23S rRNA Gene Intergenic Spacer Region ofClostridium difficile and Construction of a Library Consisting of 116 Different PCR Ribotypes. J Clin Microbiol 37:461–463.

16. Riedel T, Wetzel D, Hofmann JD, Plorin SPEO, Dannheim H, Berges M, Zimmermann O, Bunk B, Schober I, Spröer C, Liesegang H, Jahn D, Overmann J, Groß U, Neumann-Schaal M. 2017. High metabolic versatility of different toxigenic and non-toxigenic Clostridioides difficile isolates. Int J Med Microbiol 307:311–320.

17. Huang CB, Alimova Y, Myers TM, Ebersole JL. 2011. Short- and medium-chain fatty acids exhibit antimicrobial activity for oral microorganisms. Arch Oral Biol 56:650–654.

18. Zhai L, Huang C, Ning Z, Zhang Y, Zhuang M, Yang W, Wang X, Wang J, Zhang L, Xiao H, Zhao L, Asthana P, Lam YY, Chow CFW, Huang J, Yuan S, Chan KM, Yuan C-S, Lau JY-N, Wong HLX, Bian Z. 2023. *Ruminococcus gnavus* plays a pathogenic role in diarrhea-predominant irritable bowel syndrome by increasing serotonin biosynthesis. Cell Host & Microbe 31:33-44.e5.

19. Cho J, Cunningham S, Pu M, Lennon RJ, Dens Higano J, Jeraldo P, Sampathkumar P, Shannon S, Kashyap PC, Patel R. 2021. Clostridioides difficile Whole-genome Sequencing Differentiates Relapse With the Same Strain From Reinfection With a New Strain. Clin Infect Dis 72:806–813.

20. Gonzales-Luna AJ, Carlson TJ, Dotson KM, Poblete K, Costa G, Miranda J, Lancaster C, Walk ST, Tupy S, Begum K, Alam MJ, Garey KW. 2020. PCR ribotypes of *Clostridioides difficile* across Texas from 2011 to 2018 including emergence of ribotype 255. Emerg Microbes 9:341–347.

21. Snydman DR, McDermott LA, Jenkins SG, Goldstein EJC, Patel R, Forbes BA, Johnson S, Gerding DN, Thorpe CM, Walk ST. 2020. Epidemiologic trends in Clostridioides difficile isolate ribotypes in United States from 2011 to 2016. Anaerobe 63:102185.

22. Knetsch CW, Kumar N, Forster SC, Connor TR, Browne HP, Harmanus C, Sanders IM, Harris SR, Turner L, Morris T, Perry M, Miyajima F, Roberts P, Pirmohamed M, Songer JG, Weese JS, Indra A, Corver J, Rupnik M, Wren BW, Riley TV, Kuijper EJ, Lawley TD. 2018. Zoonotic Transfer of Clostridium difficile Harboring Antimicrobial Resistance between Farm Animals and Humans. J Clin Microbiol 56:e01384-17.

23. Knight DR, Kullin B, Androga GO, Barbut F, Eckert C, Johnson S, Spigaglia P, Tateda K, Tsai P-J, Riley TV. 2019. Evolutionary and Genomic Insights into Clostridioides difficile Sequence Type 11: a Diverse Zoonotic and Antimicrobial-Resistant Lineage of Global One Health Importance. mBio 10:10.1128/mbio.00446-19.

24. Kumar N, Browne HP, Viciani E, Forster SC, Clare S, Harcourt K, Stares MD, Dougan G, Fairley DJ, Roberts P, Pirmohamed M, Clokie MRJ, Jensen MBF, Hargreaves KR, Ip M, Wieler LH, Seyboldt C, Norén T, Riley TV, Kuijper EJ, Wren BW, Lawley TD. 2019. Adaptation of host transmission cycle during Clostridium difficile speciation. Nat Genet 51:1315–1320.

25. Collins J, Danhof H, Britton RA. 2019. The role of trehalose in the global spread of epidemic *Clostridium difficile*. Gut Microbes 10:204–209.

26. Pereira FC, Wasmund K, Cobankovic I, Jehmlich N, Herbold CW, Lee KS, Sziranyi B, Vesely C, Decker T, Stocker R, Warth B, von Bergen M, Wagner M, Berry D. 2020. Rational design of a microbial consortium of mucosal sugar utilizers reduces Clostridiodes difficile colonization. Nat Commun 11:5104.

27. Jenior ML, Leslie JL, Kolling GL, Archbald-Pannone L, Powers DA, Petri WA, Papin JA. 2023. Systems-ecology designed bacterial consortium protects from severe *Clostridioides difficile* infection. preprint. bioRxiv https://doi.org/10.1101/2023.08.08.552483.

28. Stein-Thoeringer CK, Nichols KB, Lazrak A, Docampo MD, Slingerland AE, Slingerland JB, Clurman AG, Armijo G, Gomes ALC, Shono Y, Staffas A, Burgos da Silva M, Devlin SM, Markey KA, Bajic D, Pinedo R, Tsakmaklis A, Littmann ER, Pastore A, Taur Y, Monette S, Arcila ME, Pickard AJ, Maloy M, Wright RJ, Amoretti LA, Fontana E, Pham D, Jamal MA, Weber D, Sung AD, Hashimoto D, Scheid C, Xavier JB, Messina JA, Romero K, Lew M, Bush A, Bohannon L, Hayasaka K, Hasegawa Y, Vehreschild MJGT, Cross JR, Ponce DM, Perales MA, Giralt SA, Jenq RR, Teshima T, Holler E, Chao NJ, Pamer EG, Peled JU, van den Brink MRM. 2019. Lactose drives *Enterococcus* expansion to promote graft-versus-host disease. Science 366:1143–1149.

29. Theriot CM, Koenigsknecht MJ, Carlson PE, Hatton GE, Nelson AM, Li B, Huffnagle GB, Z. Li J, Young VB. 2014. Antibiotic-induced shifts in the mouse gut microbiome and metabolome increase susceptibility to Clostridium difficile infection. Nat Commun 5:3114.

30. Di Rienzi SC, Britton RA. 2020. Adaptation of the Gut Microbiota to Modern Dietary Sugars and Sweeteners. Adv Nutr 11:616–629.

31. Russell C, Baker P, Grimes C, Lindberg R, Lawrence MA. 2023. Global trends in added sugars and non-nutritive sweetener use in the packaged food supply: drivers and implications for public health. Public Helath Nutr 26:952–964.

32. Glowacki RWP, Pudlo NA, Tuncil Y, Luis AS, Sajjakulnukit P, Terekhov AI, Lyssiotis CA, Hamaker BR, Martens EC. 2020. A Ribose-Scavenging System Confers Colonization Fitness on the Human Gut Symbiont Bacteroides thetaiotaomicron in a Diet-Specific Manner. Cell Host & Microbe 27:79-92.e9.

33. Girinathan BP, DiBenedetto N, Worley JN, Peltier J, Arrieta-Ortiz ML, Immanuel SRC, Lavin R, Delaney ML, Cummins CK, Hoffman M, Luo Y, Gonzalez-Escalona N, Allard M, Onderdonk AB, Gerber GK, Sonenshein AL, Baliga NS, Dupuy B, Bry L. 2021. In vivo commensal control of Clostridioides difficile virulence. Cell Host & Microbe 29:1693-1708.e7.

34. Shaw HA, Preston MD, Vendrik KEW, Cairns MD, Browne HP, Stabler RA, Crobach MJT, Corver J, Pituch H, Ingebretsen A, Pirmohamed M, Faulds-Pain A, Valiente E, Lawley TD, Fairweather NF, Kuijper EJ, Wren BW. 2020. The recent emergence of a highly related virulent Clostridium difficile clade with unique characteristics. Clin Microbiol Infect 26:492–498.

35. Eyre DW, Didelot X, Buckley AM, Freeman J, Moura IB, Crook DW, Peto TEA, Walker AS, Wilcox MH, Dingle KE. 2019. Clostridium difficile trehalose metabolism variants are common and not associated with adverse patient outcomes when variably present in the same lineage. EBioMedicine 43:347–355.

36. Shaw HA, Khodadoost L, Preston MD, Corver J, Mullany P, Wren BW. 2019. Clostridium difficile clade 3 (RT023) have a modified cell surface and contain a large transposable island with novel cargo. Sci Rep 9:15330.

37. Battaglioli EJ, Hale VL, Chen J, Jeraldo P, Ruiz-Mojica C, Schmidt BA, Rekdal VM, Till LM, Huq L, Smits SA, Moor WJ, Jones-Hall Y, Smyrk T, Khanna S, Pardi DS, Grover M, Patel R, Chia N, Nelson H, Sonnenburg JL, Farrugia G, Kashyap PC. 2018. *Clostridioides difficile* uses amino acids associated with gut microbial dysbiosis in a subset of patients with diarrhea. Sci Transl Med 10:eaam7019.

518 38. Aguirre AM, Yalcinkaya N, Wu Q, Swennes A, Tessier ME, Roberts P, Miyajima F, Savidge T, Sorg JA.
519 2021. Bile acid-independent protection against Clostridioides difficile infection. PLoS Pathog
520 17:e1010015.

521 39. Bouillaut L, Self WT, Sonenshein AL. 2013. Proline-Dependent Regulation of Clostridium difficile Stickland
522 Metabolism. J Bacteriol 195:844–854.

523 40. Gencic S, Grahame DA. 2020. Diverse Energy-Conserving Pathways in Clostridium difficile: Growth in the
524 Absence of Amino Acid Stickland Acceptors and the Role of the Wood-Ljungdahl Pathway. J Bacteriol
525 202.

526 41. Karasawa T, Ikoma S, Yamakawa K, Nakamura S. 1995. A defined growth medium for Clostridium difficile.
527 Microbiology 141:371–375.

528 42. Midani FS, Collins J, Britton RA. 2021. AMiGA: Software for Automated Analysis of Microbial Growth
529 Assays. mSystems 6:e0050821.

530 43. Subramanian A, Tamayo P, Mootha VK, Mukherjee S, Ebert BL, Gillette MA, Paulovich A, Pomeroy SL,
531 Golub TR, Lander ES, Mesirov JP. 2005. Gene set enrichment analysis: A knowledge-based approach for
532 interpreting genome-wide expression profiles. Proceedings of the National Academy of Sciences
533 102:15545–15550.

534 44. Fang Z, Liu X, Peltz G. 2023. GSEApy: a comprehensive package for performing gene set enrichment
535 analysis in Python. Bioinformatics 39:btac757.

536

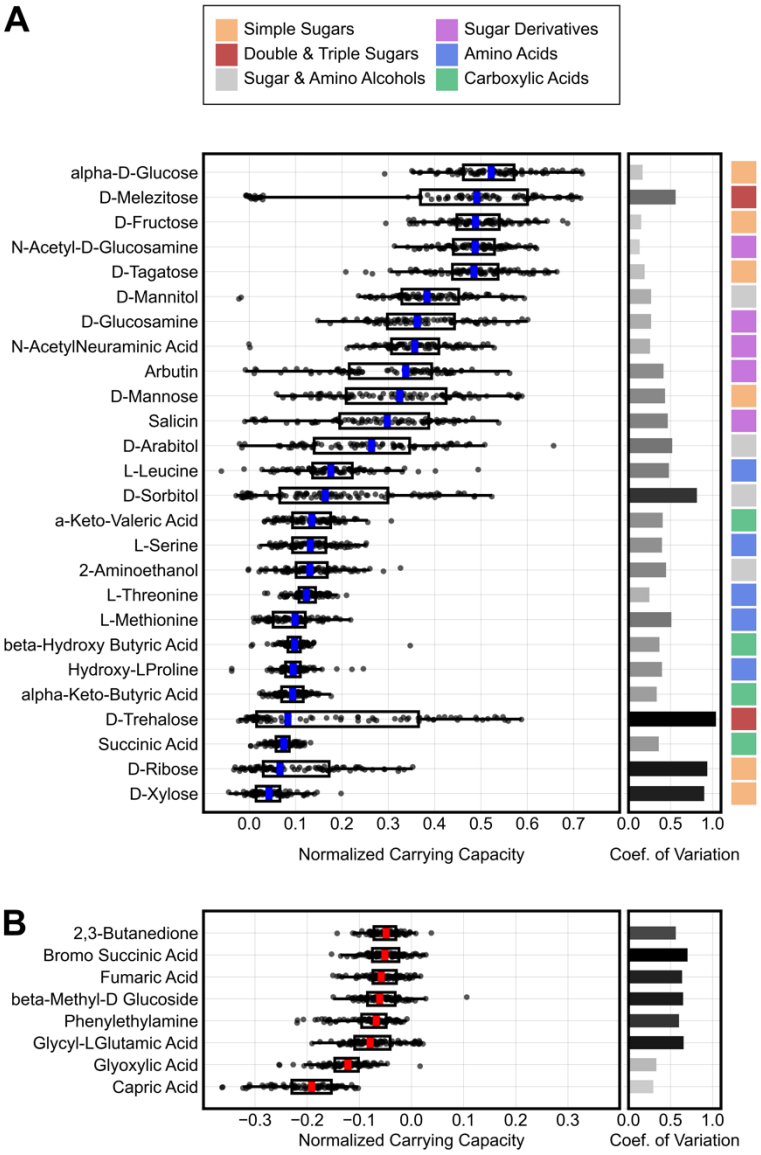

Figure 1. *C. difficile* is a generalist species that grows on a variety of carbon sources. (A) Plot displays the normalized carrying capacity for 88 *C. difficile* isolates on the top 26 most commonly used substrates. Normalized carrying capacity is defined as the optical density (OD) on minimal media supplemented with a single carbon source beyond the OD of growth on minimal media alone. **(B)** Bottom panel display carbon sources that inhibited growth. Box plots display the median and interquartile range of values. Whiskers extend to the farthest point within 1.5x of the interquartile range. Horizontal bars on the right side display the coefficients of variation for each distribution and the shading of these bars scales with the coefficient's value. For inhibitory substrates, coefficients of variation were computed on -1x normalized carrying capacity. Top legend maps each substrate to a chemical group.

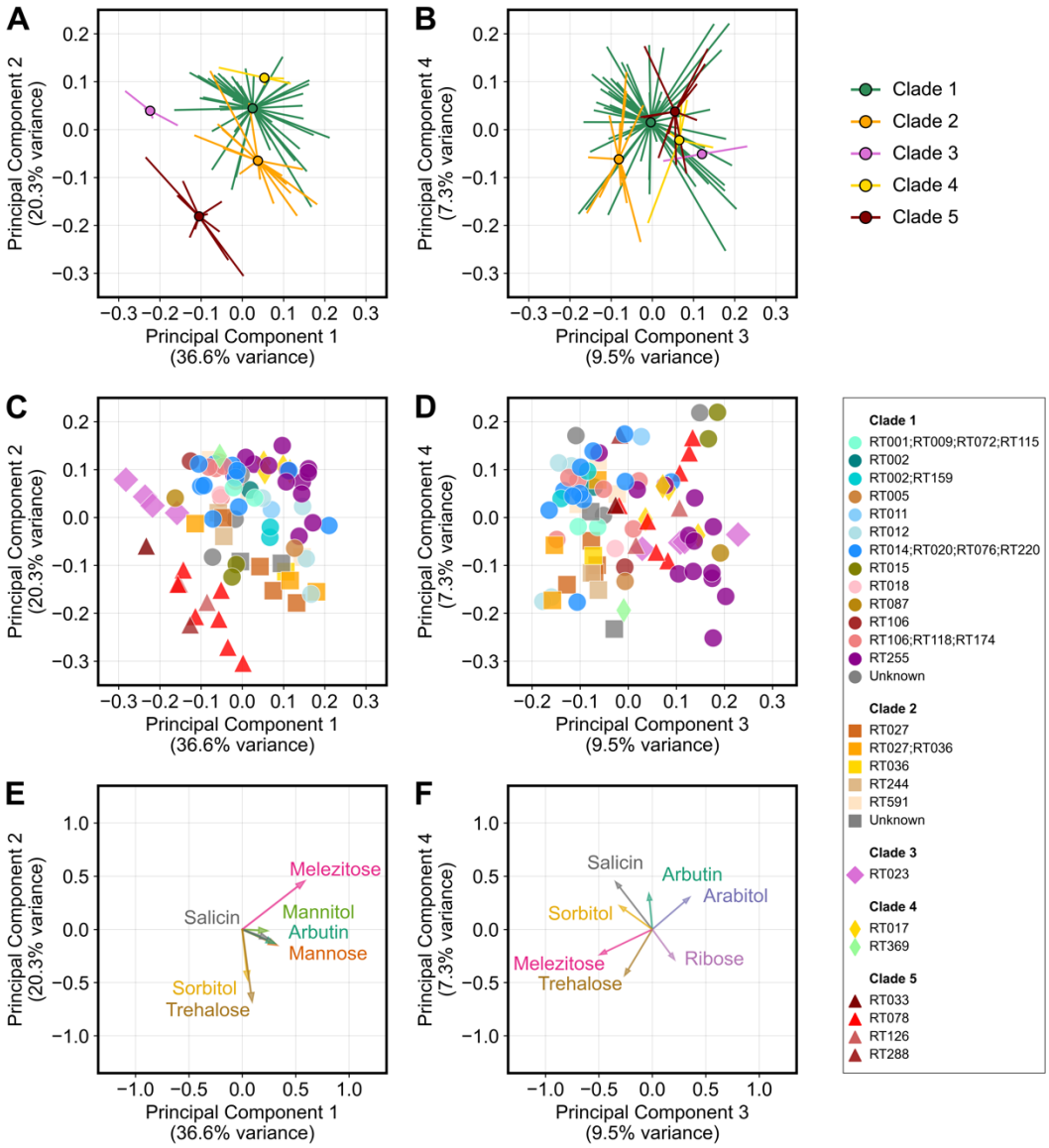

Figure 2. Isolates cluster by phylogenetic clade and molecular ribotype based on their growth on carbon sources. (**A**-**B**) Top panels display the principal component analysis of the growth of isolates on the top 26 carbon substrates. Isolates are grouped by clades with circles indicating the centroid for each group and lines pointing to the location of each isolate in the ordination plots. (**C**-**D**) Middle panels display the same principal component analysis, and further delineate the ribotype of each isolate with colors and clade with shapes, as indicated in the legend on the right. (**E**-**F**) Bottom panels visualize how certain substrates contribute to the position of isolates on the principal components (loading factors). Left column displays analysis for the first and second principal components while the right column displays analysis for the third and fourth principal components.

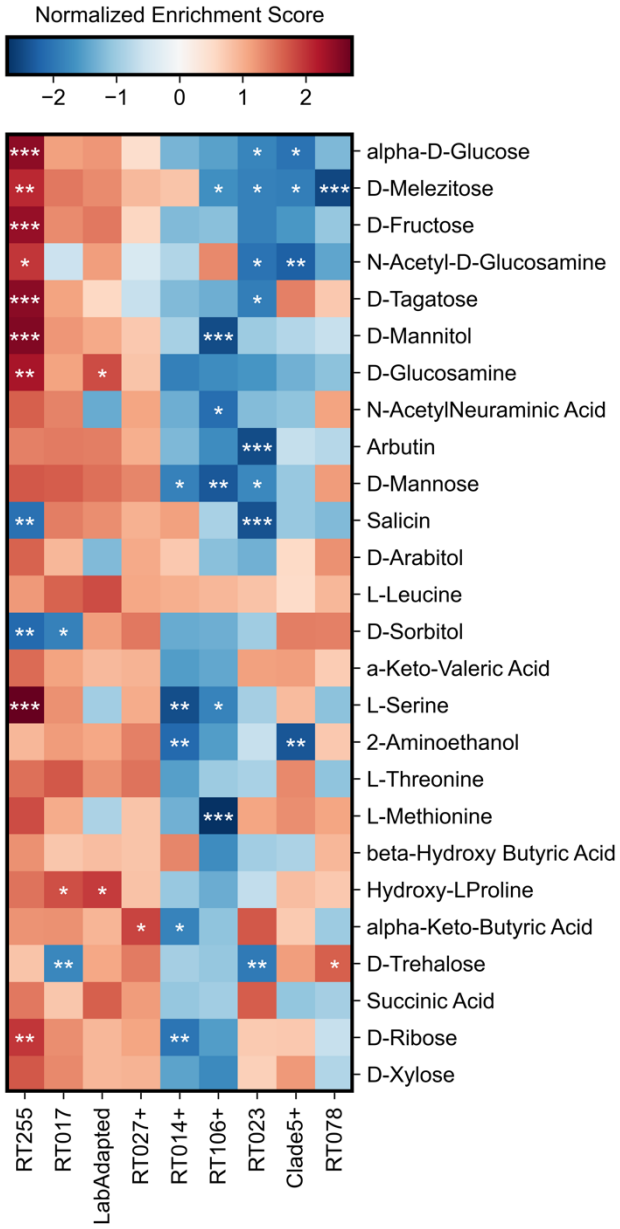

Figure 3. Emerging and epidemic *C. difficile* ribotypes exhibit unique metabolic phenotypes. Heatmap displays which ribotypes are positively or negatively enriched for growth on each of the top carbon sources. Normalized enrichment scores were computed using strain set enrichment analysis. Strain groups (columns) are hierarchically clustered based on similarity of their normalized enrichment scores, while substrates (rows) are ordered from top to bottom based on the median growth of all isolates as shown in Figure 1. For each substrate, statistical significance was estimated with a permutation-based test procedure and corrected with the Benjamini-Hochberg method. **P* < 0.05, ***P* < 0.01, ****P* < 0.001.

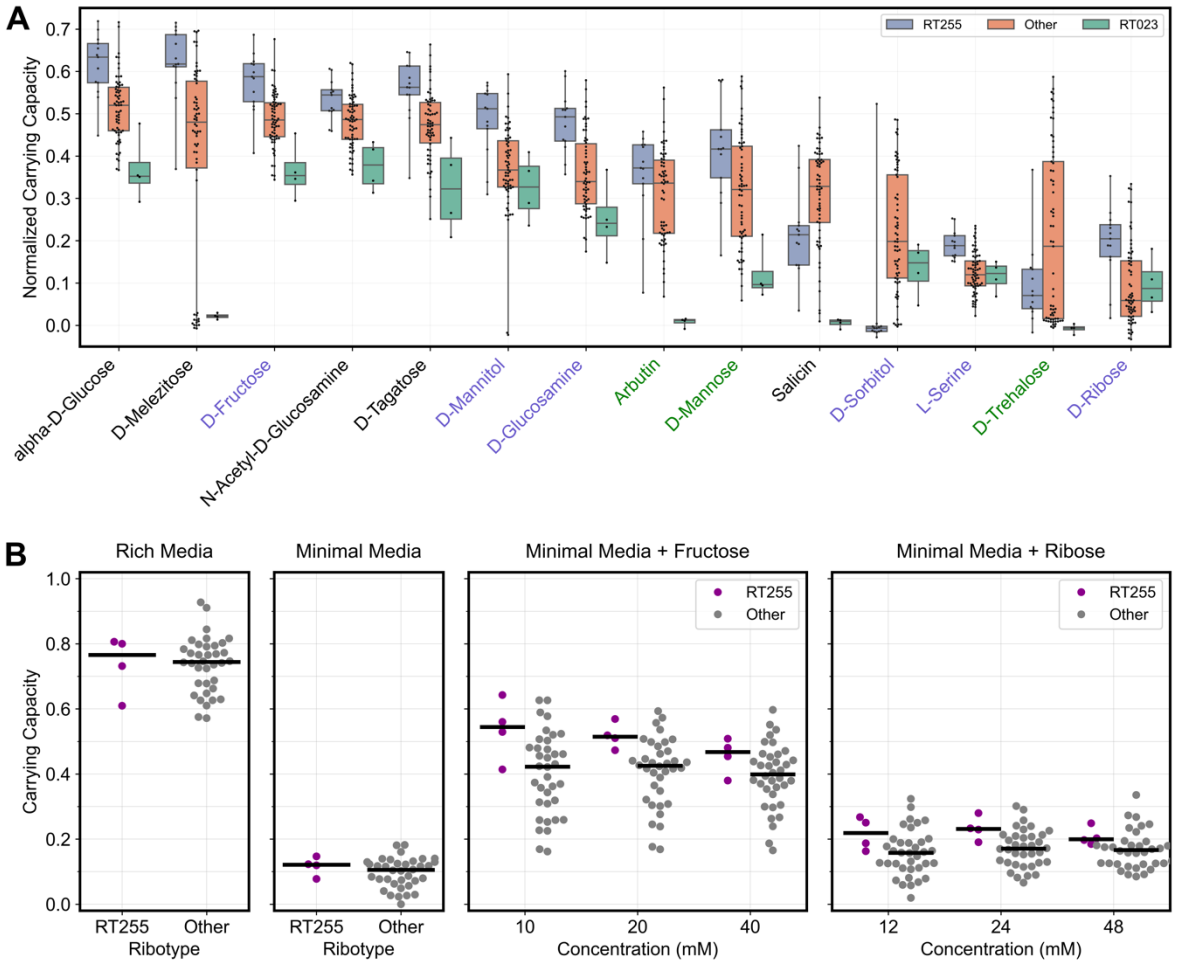

562 **Figure 4. Emerging *C. difficile* ribotypes have divergent metabolic phenotypes.** (**A**) Based on Biolog
563 Phenotype Microarray assays, ribotypes 255 and 023 were significantly enriched or depleted in growth on a
564 combined total of 14 substrates ($P < 0.05$, strain set enrichment analysis). Black text labels indicate substrates
565 that differentially impacted growth for both ribotypes 255 and 023. Blue and green text labels indicate
566 substrates that differentially impacted growth for only ribotype 255 or ribotype 023 respectively. Whiskers span
567 the range of each distribution from lowest to highest value. **(B**) In validation experiments, "RT255" isolates
568 reached significantly higher carrying capacity on fructose and ribose than isolates belonging to "other"
569 ribotypes. *C. difficile* isolates harvested during exponential growth were inoculated into minimal media
570 supplemented with either fructose or ribose at the indicated concentrations. As controls, we display the growth
571 of isolates on minimal and rich media. Each data point represents the average of technical duplicates. Using
572 likelihood tests on linear mixed effects models, we found that both ribotype identity (RT255 or Other) and
573 interaction of ribotype identity with substrate (fructose, ribose, or none) improved model performance ($P <$
574 0.05).

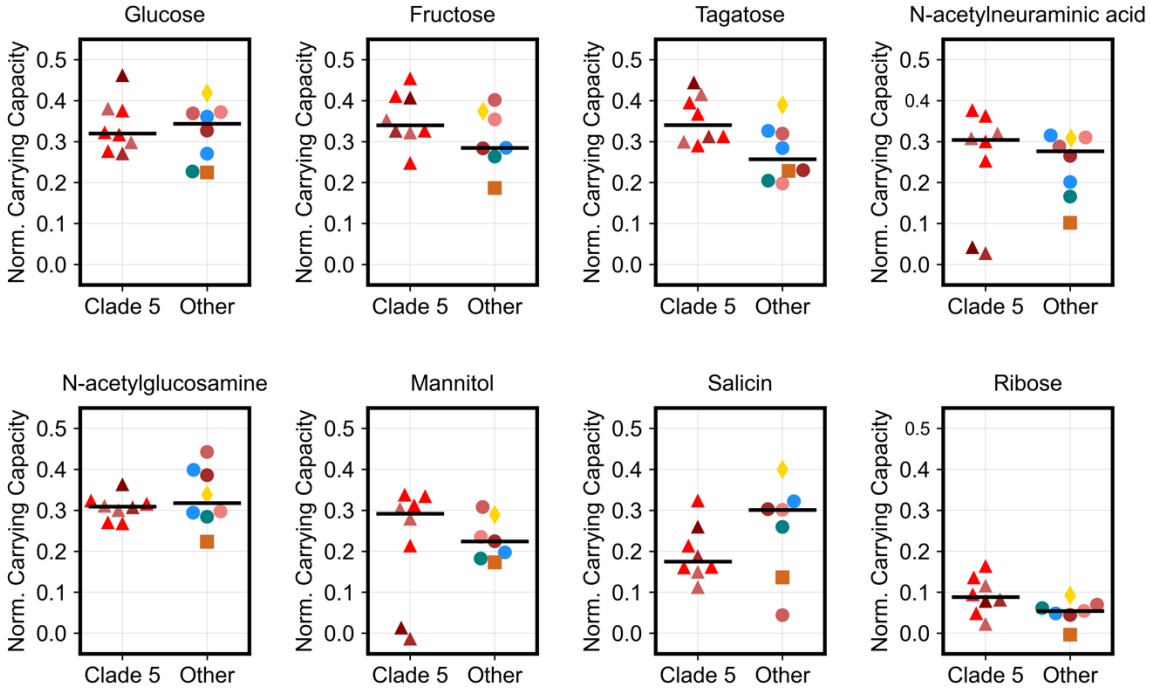

Figure 5. Clade 5 ribotypes grow more robustly on simple sugars than Clade 1-4 ribotypes. *C. difficile* isolates harvested during exponential growth were inoculated into minimal media supplemented with one of eight different carbon substrates, including the simple sugars glucose, fructose, tagatose, and ribose. Strip plots visualize the normalized carrying capacity or the additional growth for each isolate on each carbon source beyond baseline growth on minimal media. Colors and markers indicate the ribotype and clade of each isolate as shown in Figure 2. Clade 5 isolates included ribotypes 078, 033, 126, and 288. Additional isolates tested belonged to ribotypes 001, 002, 014-020, 017, 027, and 053. Substrates were ordered from left to right by median growth of all isolates as shown in Figure 1. Each data points represents average of technical duplicates. Using likelihood tests on linear mixed effects models, we found that interaction of clade identity (Clade 5 or Other) with substrate type (simple sugar vs other sugar) improved model performance ($P < 0.001$).

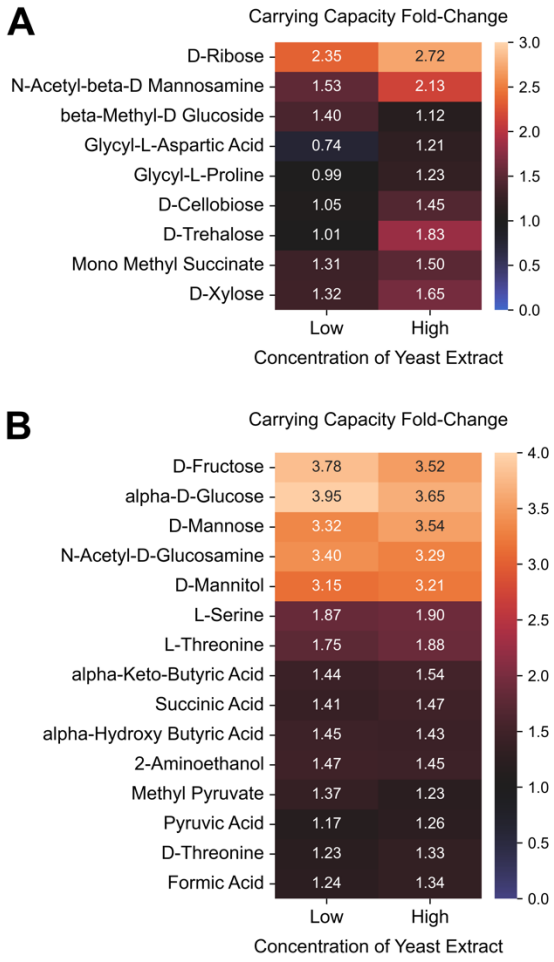

Figure 6. Ribotype 017 isolate grow on trehalose and cellobiose only if pre-cultured on media with high yeast extract. *C. difficile* strain M68 was profiled for growth in a Biolog PM1 plate after pre-culturing overnight in brain heart infusion with either low (0.5%) or high (5%) yeast extract. Heatmaps display the fold-change for carrying capacity on minimal media supplemented with each substrate relative to carrying capacity on minimal media only. (**A-B**) All displayed substrates supported the growth of M68 with fold-change values of at least 1.2 on either or both of the yeast extract concentrations. (**A**) Heatmap displays only the substrates with fold-change values for growth on high yeast extract that were at least 10% higher or lower than fold-change values for growth on low yeast extract, while (**B**) heatmap displays the remaining substrates. For each heatmap, substrates were ordered by agglomerative hierarchical clustering of fold-change values using UPGMA.

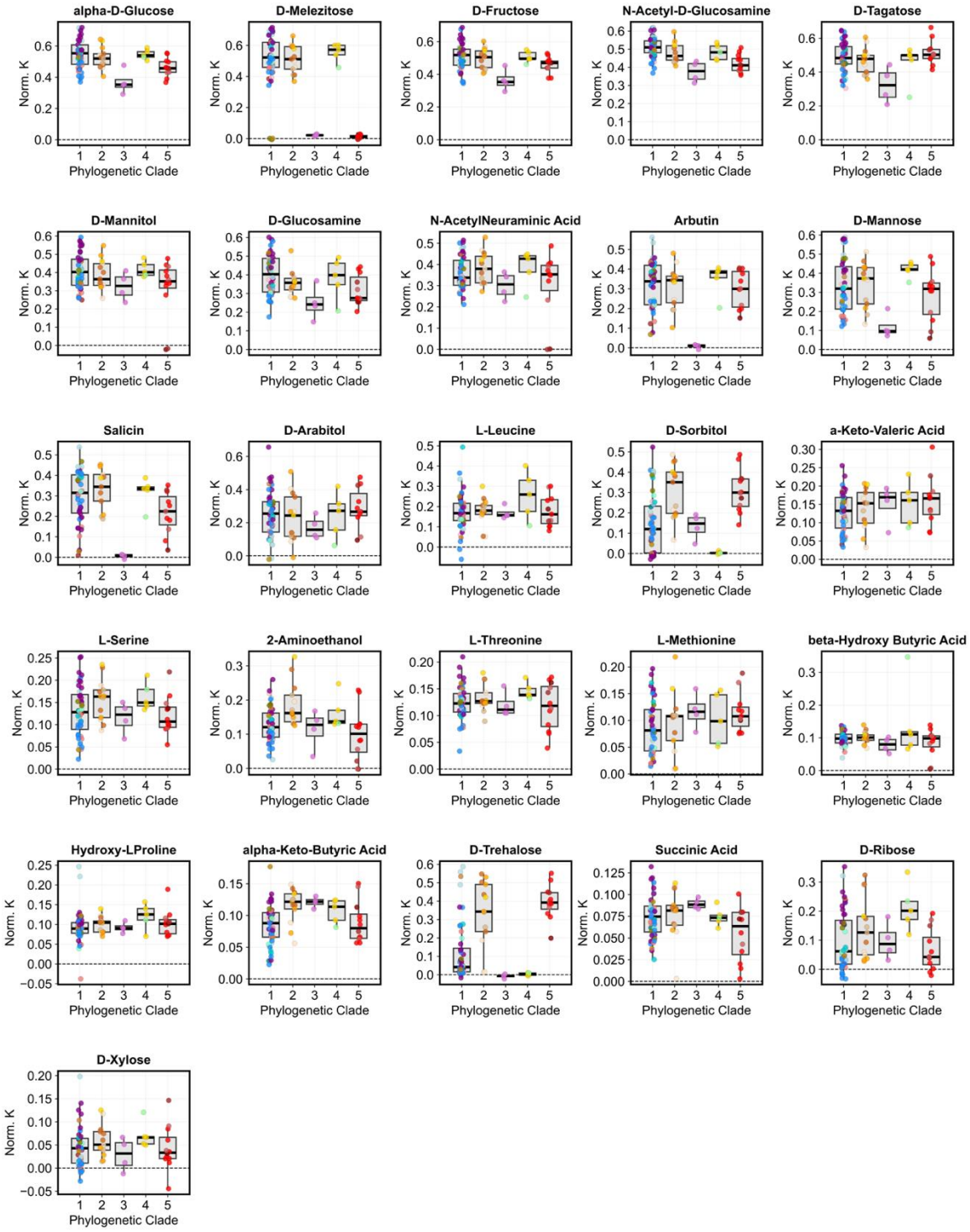

Figure S1. Normalized carrying capacity (K) for all isolates on the top carbon sources. Colors and markers indicate the ribotype and clade of each isolate as shown in Figure 2. Whiskers extend to the farthest point within 1.5x of the interquartile range.

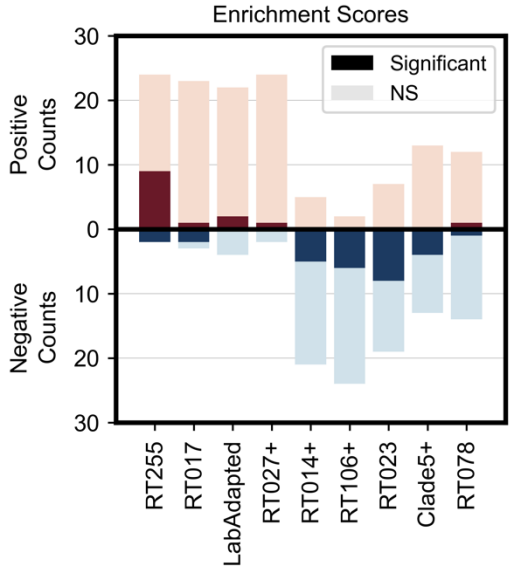

Figure S2. Summary chart for the strain set enrichment analysis shown in Figure 3. Bars display the total count of positive enrichments (red bars) and negative enrichments (blue bars) for each ribotype. Dark and light shading indicates enrichments that are statistically significant or not significant (NS), respectively.

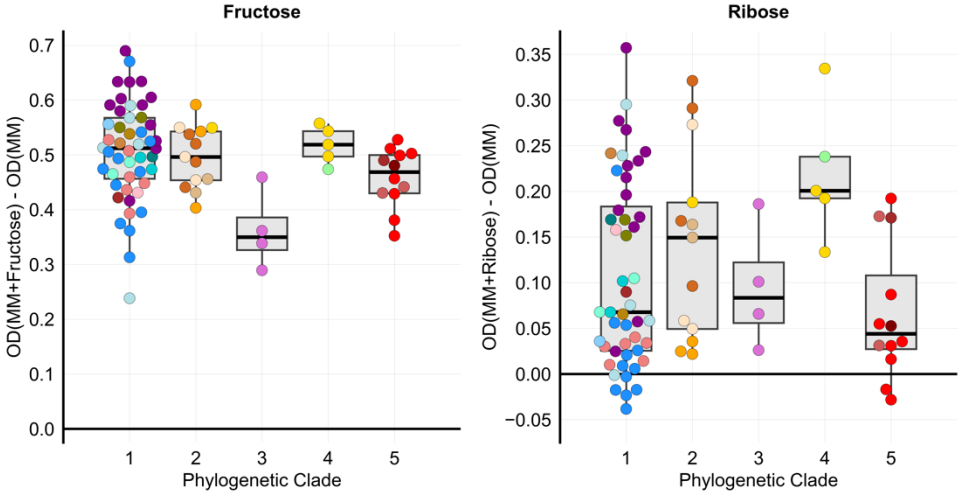

Figure S3. Normalized carrying capacities for isolates grown on minimal media supplemented with either fructose or ribose in the Biolog Phenotype Microarray plates. Colors and markers indicate the ribotype and clade of each isolate as shown in Figure 2. Ribotype 255 isolates are marked by purple circles in Clade 1. OD: Optical density; MM: Minimal Media.

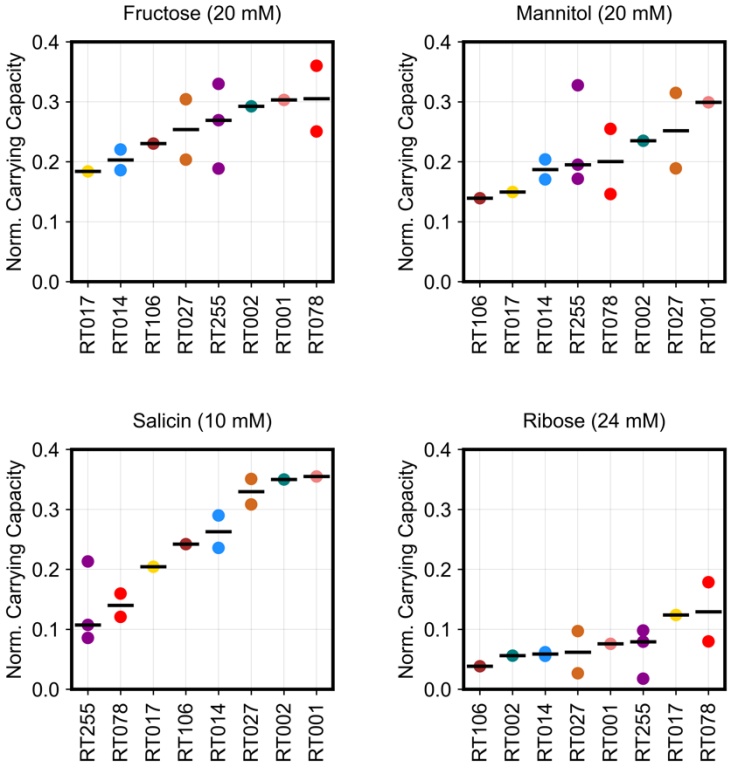

Figure S4. Growth validation experiment recapitulated patterns detected by the Biolog phenotype microarray assays. *C. difficile* harvested during exponential growth was inoculated into minimal media with one of four carbon substrates. Colors indicate the ribotype of each isolate as shown in Figure 2.

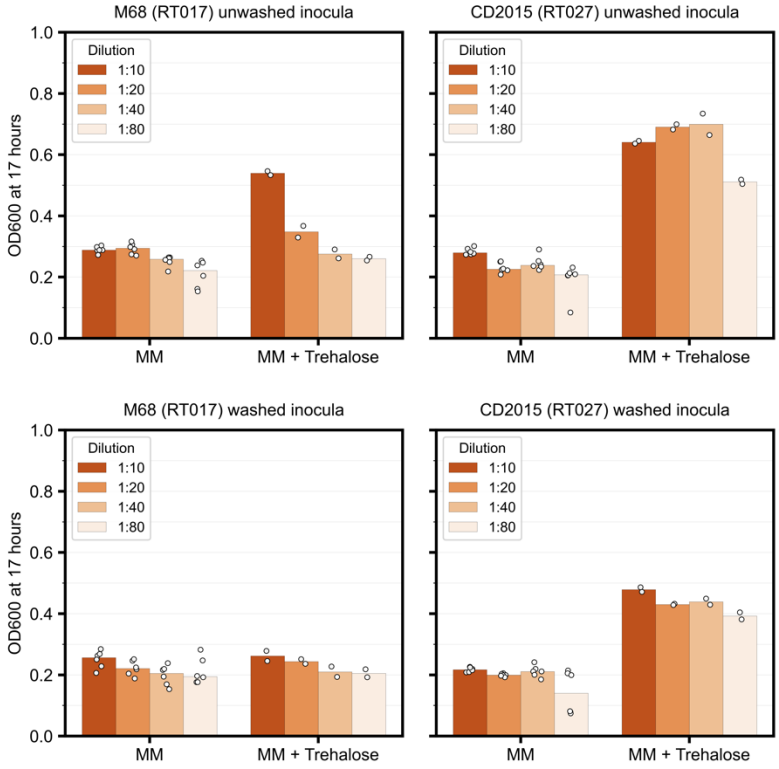

Figure S5. Unknown limiting factor in yeast extract enabled ribotype 017 to grow on trehalose. Ribotype 017 isolate M68 and ribotype 027 isolate CD2015 were grown overnight in brain heart infusion supplemented with high yeast extract, serially diluted in defined minimal media, then grown on minimal media (MM) alone or minimal media supplemented with 40 mM trehalose. Overnight cultures were either washed in defined minimal media, or not, prior to dilution and inoculation. Left and right panels display results for M68 and CD2015 respectively. Top and bottom panels display results for growth using unwashed and washed inocula respectively. Using unwashed inocula, the maximum optical density of M68 on trehalose decreased with increasing dilution factors which suggests that a limiting factor is necessary for growth on trehalose. In addition, M68 was unable to grow on trehalose after washing likely because washing eliminated this limiting factor.

SUPPLEMENTAL TABLE LEGENDS

Table S1. Sources of *C. difficile* isolates.

Table S2. Molecular typing of *C. difficile* isolates.

Table S3. Composition of *C. difficile* minimal media.